BROWNIAN MOTION IN A PERIODIC POTENTIAL: APPLICATION TO DIELECTRIC RELAXATION

by

Fabio Marchesoni
Dublin Institute for Advanced Studies,
10 Burlington Road, DUBLIN 4 (Éire)

and

Jagdish K. Vij
Department of Microelectronics and Electrical Engineering,
Trinity College, DUBLIN 2 (Éire)

submitted to Z. Phys. B August 1984

ABSTRACT

The relaxational dynamics of a planar rotator in an M-fold cosine potential subject to a random torque is investigated in detail. For the case of a periodic potential with large barrier height, the numerical results the relaxation dynamics are in complete agreement with an approximate analytic solution. The latter is derived on assuming a harmonic potential at the bottom of the potential minima and a large time-scale separation between the short-time libration inside each potential minima and a long-time hopping phenomenon over the potential barriers. For $M \gg 2$, the hopping phenomenon is found to be the dominant feature of the orientational auto-correlation function. The average hopping time is explained satisfactorily in terms of the Kramers activation rate theory. In particular a complete agreement is found between the numerical results of the escape rate and those obtained from the modified Kramers' predictions valid for low friction coefficient. The cosine model is applied to the study of dielectric spectroscopy. The particle mobility and the complex permittivity of a dielectric material are calculated by numerical solutions for rotational velocity and orientational auto-correlation functions, respectively. The main features of the experimental observables are determined analytically and compared to the corresponding numerical results. The applicability of the plane rotator model to dielectric spectroscopy is also discussed.

1 INTRODUCTION

The present paper is aimed at developing in more detail the applications of the one-dimensional brownian motion in an M-fold cosine potential introduced by Dieterich et al /1,2/ and Risken and Vollmer /3,4/. An earlier attempt by Dianoux and Volino /5/ deals with the problem of diffusion in a periodic potential by disregarding the inertial effects. These treatments are based on the Fokker-Planck equation (FPE) formalism. In ref 5 many analytic results are given due to the simpler structure of the corresponding one-variable (displacement x (t)) FPE. In refs 3 and 4 the two-variable FPE (in x (t) and $\dot{x}$ (t)) is reduced to a set of differential-difference equations and then integrated numerically, whereas in refs 1 and 2 calculations are done using the continued fraction expansion of the relevant statistical auto-correlation functions (acf). Despite the fact that the latter technique has produced reliable results through comparatively fast computer algorithms /6,7/ the rapid convergence of the expansion introduced in ref 3 enables us to explore the dynamics of the brownian motion in a sinusoidal potential over a wide range of parameters.

The algorithm used in the present paper is due to Reid/8/ . The algorithm allows a detailed numerical discussion of the relaxational dynamics of the model by computing the Laplace (Fourier) transform of relevant acf's. A detailed derivation of the basic differential-difference equations used in ref 8 have been recently reviewed by Risken /9/ and Coffey et al /10/.

Our approach to the problem under investigation has been inspired by the conclusions of a previous analysis by Praestgaard and van Kampen /11/. They have shown that in the case of an M-fold periodic potential a large separation between short and long-time relaxation process can occur provided that the thermal (activating) energy k_BT is small compared to the activation energy (or barrier height) ΔV. The features of the phenomena of resonance (or libration can then be distinguished from those of the diffusion (or hopping) process.

Our main conclusion is that the numerical results give a convincing evidence for the analytical results of the outlying picture of brownian motion presented in ref 11. For the case of high activation energy ($\Delta V \gg k_BT$), the orientational relaxation within an M-fold periodic potential with $M > 1$ turns out to be a diffusive process even in the underdamped limit. The time scale of the latter process can be related to the activation time - defined as the average time needed for the brownian particle to reach the top of the barrier. The Kramers' approach to relaxational processes /12,13/ therefore proves to be a powerful tool for calculating the diffusional physical quantities of the system.

A great variety of physical phenomena in condensed matter have been modelled by a number of authors /2,4,9-11/ on the basis of the one-dimensional motion in a periodic potential. Following Reid /8/ and also Praestgaard and van Kampen /11/ we apply this model to dielectric spectroscopy. The model assumes that the molecule has M equivalent stable orientations, ie M potential minima of the orientations. These minima are separated by similar potential barriers whose heights ΔV are larger than k_BT. The molecule librates about one of these minima, subject to damping (with frictional coefficient β) and a random torque $\tau(t)$, representing the neighbouring molecules to a first approximation.

For a two-dimensional system (planar rotator) with moment of inertia I, temperature T and orientation θ, the equation of motion is:

$$\dot{\vartheta} = \omega$$
$$I\dot{\omega} = -\beta I\omega - V'(\vartheta) + \tau(t) \qquad (1.1)$$

where the Langevin torque $\tau(t)$ is assumed to be gaussian white noise with

$$\langle \tau(t) \rangle \equiv 0 \ , \quad \langle \tau(t)\tau(0) \rangle = 2 k_B T \beta I \delta(t) \ . \qquad (1.2)$$

We assume potential $V(\vartheta)$ to be:

$$V(\vartheta) = -V_0 \cos(M\vartheta) \ . \qquad (1.3)$$

The corresponding FPE can be rewritten as:

$$\frac{\partial}{\partial t} \rho = -\omega \frac{\partial}{\partial \vartheta} \rho + M \gamma \alpha \sin(M\vartheta) \frac{\partial}{\partial \omega} \rho + \beta \left(\frac{\partial}{\partial \omega} \omega + \alpha^2 \frac{\partial^2}{\partial \omega^2} \right) \rho \ , \qquad (1.4)$$

where the adopted notation is as follows:

$$\alpha^2 = k_B T / I \ , \quad \gamma = V_0 / I\alpha \ . \qquad (1.5)$$

ρ is the transition probability density $\rho(\vartheta, \omega; t | \vartheta(0), \omega(0); 0)$ of the process with delta function initial conditions:

$$\rho(\vartheta, \omega; 0) = \delta(\vartheta(0) - \vartheta_0) \, \delta(\omega(0) - \omega_0) \ . \qquad (1.6)$$

The equilibrium probability distribution is given by

$$\rho_{eq}(\vartheta, \omega) = \mathcal{N} \exp\left(-\omega^2 / 2\alpha^2\right) \exp\left(\gamma/\alpha \cos(M\vartheta)\right) \ ,$$

where $\mathcal{N}$ is a normalization constant.

Of course we pretend not to describe the details of an actual complicated many-body process by employing such a simple model. In particular the non-markovian statistics of the heat bath simulating the surroundings have been proven to affect greatly the relaxational properties of dielectric samples subject to external electric fields /14/. The qualitative predictions obtained from the model so far, however, do explain satisfactorily a wide variety of experimental and numerical observations /8,10/.

To analyze the model of eq (1.1) we are interested in the following acf's:

(i) The mobility or conductivity spectra of particles undergoing rotational motion in an M-fold potential, given by the following equation

$$\mu(\omega) = \mathrm{Re} \left\{ \frac{1}{\alpha^2} \int_0^\infty e^{-i\omega t} \langle \omega(t)\omega(0) \rangle_{eq} \, dt \right\} \ . \qquad (1.8)$$

Here $\langle \ldots \rangle_{eq}$ denotes the average evaluated under equilibrium (Maxwell--Boltzmann) initial conditions and notation is as in eq. (1.4). $\mu(\omega)$ is the cosine Fourier transform of the rotational velocity equilibrium acf :

$$C_{eq}(t) \equiv \langle \omega(t)\omega(0) \rangle_{eq} / \langle \omega^2 \rangle_{eq} \ . \qquad (1.9)$$

From eq (1.7) $\quad \langle \omega^2 \rangle_{eq} = k_B T / I = \alpha^2 \ .$

(ii) The equilibrium orientational acf of the rotating molecule

$$K_{eq}(t) = \frac{\langle \cos\vartheta(t) \cos\vartheta(0) \rangle_{eq} - \langle \cos\vartheta(0) \rangle^2_{eq}}{\langle \cos^2\vartheta(0) \rangle_{eq} - \langle \cos\vartheta(0) \rangle^2_{eq}} \ . \qquad (1.10)$$

The complex permittivity is related to the orientational correlation (in the absence of internal field corrections) by /15/:

$$\varepsilon^*(\omega) = \varepsilon'(\omega) - i\varepsilon''(\omega) = \varepsilon_\infty + (\varepsilon_s - \varepsilon_\infty) \left[1 - i\omega \cdot \int_0^\infty e^{-i\omega t} \langle \cos\vartheta(t) \cos\vartheta(0) \rangle_{eq} \, dt \right] \ , \qquad (1.11)$$

where ε_s and ε_∞ denote the static and infinite frequency permittivities, respectively. The power absorption (in the far infrared (IR)) is given by /15/:

$$\alpha(\omega) = \omega \varepsilon''(\omega) / nc \ , \qquad (1.12)$$

where n is the refractive index and c is the velocity of light in vacuo

The plan of this paper is as follows. In Section 2 we discuss our results for the mobility. The static mobility, $\mu(0)$, is related to the translational diffusional coefficient and compared with Kramers' predictions of the latter for both the overdamped and underdamped limit. Recent results /16/ for the relaxation in the underdamped limit are tested successfully. Effects due to the non-linear nature of the potential show up clearly when the dependence of the dynamic mobility, $\mu(\omega)$, on frequency is investigated. The results on the dielectric loss, $\varepsilon''(\omega)$, are discussed in Section 3. We find that in the limit of high activation energies ($\Delta V \gg k_B T$) the approximate

solution of ref 11 for $K_{eq}(t)$ is shown to explain satisfactorily the dependence of low-frequency $\varepsilon''(\omega)$ on the model parameters. In particular the loss peak for $M > 1$ is related to the diffusional (long-time) features of the system. Shorter-time phenomena (ie. libration) can also be revealed on resolving the higher frequency details of the orientational spectrum, especially through the power absorption spectrum, $\alpha(\omega)$. Finally, in Section 4 we summarize our findings and discuss their experimental implications.

2 PARTICLE MOBILITY

Firstly, we compare results obtained from our algorithms with those reported in refs 1 and 2 to test its effectiveness. The case, not covered by previous analyses, when the activation energy is comparable to the thermal energy ($\Delta V \sim k_B T$) especially for a small friction coefficient, β, is investigated in detail. For this discussion $M = 1$ and the notation is as reported in Introduction. As a consequence, the effects due to the hopping dynamics are under better control and a comparison with the Kramers' thermal activation theory is made easier.
Reid's algorithm is reviewed briefly in Appendix A.

(a) static mobility

The static mobility $\mu(0)$ can be defined as the $s = 0$ value of the Laplace transform $\mathcal{L}\{C_{eq}(t)\} = \hat{C}_{eq}(s)$ (see eqs. (1.8) and (1.9)).
Moreover $\mu(0)$ can be easily related to the translational diffusion constant D. The Laplace transform of the translational acf, $\langle \vartheta(t)\vartheta(0)\rangle_{eq}$, can readily be worked out:

$$\mathcal{L}\{\langle \vartheta(0)\ \ \dot{\vartheta}(0) - \dot{\vartheta}(t)\rangle_{eq}\} = \frac{1}{s}\langle \vartheta(0)\ \ \dot{\vartheta}(0) - s\hat{\vartheta}(s)\rangle_{eq} = -\frac{1}{s}\langle \vartheta(0)\,\hat{\omega}(s)\rangle_{eq} =$$
$$= \frac{1}{s}\langle \omega(0)\,\hat{\vartheta}(s)\rangle_{eq} = \frac{1}{s^2}\mathcal{L}\{\langle \omega(t)\omega(0)\rangle_{eq}\} = \frac{1}{s^2}\alpha^2\hat{C}_{eq}(s). \tag{2.1}$$

The $s = 0$ value of $\langle \hat{\omega}(s)\hat{\omega}(0)\rangle_{eq}$ is therefore the linear term (with a change of sign) in the time expansion of $\langle \vartheta(t)\vartheta(0)\rangle_{eq}$. This is the well-known Einstein relation /15/, see eq (1.8),

$$D = \alpha^2 \mu(0). \tag{2.2}$$

In order to prove that D is related to the escape process from the (single) potential well and that it can be interpreted in terms of the Kramers' activation theory, approximate analytical expressions for the normalized

acf of $\vartheta(t)$ and $\omega(t)$ are given. Following Praestgaard and van Kampen approach, we assume that for high enough activation energy ($\gamma > \alpha$), a clearcut time scale separation occurs between a damped oscillatory motion about the bottom of the well and a rare hopping process over the barrier. If $\varkappa$ denotes the rate of escape from the well, such an assumption implies that $\varkappa$ is much longer than the inverse of the damping time, β, as well as the approximate resonance frequency $\sqrt{\gamma\alpha}$. Indeed we can describe the former process in the linear approximation of potential while the latter using the Kramers' approach.

Following the above arguments, let

$$V(\vartheta) = \Omega_0 I \left(\vartheta^2/2 - 1 \right) \qquad \text{with} \qquad \Omega_0^2 = \gamma\alpha \, .$$

After some easy algebra /11,13/ we obtain (see Appendix B):

$$C_L(t) = e^{-\varkappa t} \mathcal{U}_\omega(t) \tag{2.3}$$

$$R_L(t) \equiv \langle \vartheta(t)\vartheta(0) \rangle / \langle \vartheta^2(0) \rangle = e^{-\varkappa t} \mathcal{U}_\vartheta(t) \, , \tag{2.4}$$

where

$$\mathcal{U}_\omega(t) = e^{-\frac{\beta}{2}t} \left[\cos \Omega t - \frac{\beta}{2\Omega} \sin \Omega t \right] \tag{2.5}$$

$$\mathcal{U}_\vartheta(t) = e^{-\frac{\beta}{2}t} \left[\cos \Omega t + \frac{\beta}{2\Omega} \sin \Omega t \right] \tag{2.6}$$

with

$$\Omega^2 = \Omega_0^2 - \beta^2/4 \, . \tag{2.7}$$

It is to be noted that in the linear approximation (denoted by the subscript L) the acf's do not depend on the initial conditions. Using the energy equipartition relation (rigorous in the linear approximation), $\langle \vartheta^2 \rangle = \langle \omega^2 \rangle / \gamma\alpha = \alpha/\gamma$, eq (2.1) can be rewritten as

$$\hat{R}_L(s) = \frac{1}{s^2} \left\{ \gamma\alpha \, \hat{C}_L(s) \right\} , \tag{2.8}$$

where $\hat{C}_L$ is given by

$$\hat{C}_L(s) = (s+\varkappa) \Big/ \left[(s+\varkappa)^2 + \beta(s+\varkappa) + \gamma\alpha \right] . \tag{2.9}$$

The translational diffusional constant (by definition the $s = 0$ value of the factor between braces in eq (2.8)) is then approximated by $\varkappa$, ie $D \sim \varkappa$. On the other hand we can easily check that the linear term (with a change of sign) in the time expansion of $R_L(t)$ is just $\varkappa$.

We calculate now the rate $\varkappa$ by applying the thermal activation theory /12, 13, 16, 17/. Let us consider the brownian motion about a metastable potential minimum A. In the case when only one escape path through B is allowed and the jump over the barrier B (with height ΔV) is irreversible, the Kramers' predictions for the activation (escape) rate η_1 lead to

$$\eta_1 = \frac{\omega_A}{2\pi |\omega_B|} \left[\left(\frac{\beta^2}{4} + \omega_B \right)^{\frac{1}{2}} - \frac{\beta}{2} \right] \cdot \exp\left(-\Delta V / k_B T \right) , \tag{2.10}$$

(for large to intermediate values of β /12,13/)

$$\eta_1 = \beta \, \frac{\Delta V}{k_B T} \cdot \exp\left(-\Delta V / k_B T \right) \, . \tag{2.11a}$$

(for small values of β /12/)

where ω_A and ω_B are the quadratic terms of the potential expansion around A and B respectively. Recently Büttiker et al /16/ produced a more refined estimate for the underdamped limit of η_1:

$$\eta_1 = \frac{4\beta}{\pi} \, \frac{\Delta V}{k_B T} \exp\left(-\Delta V / k_B T \right) \, . \tag{2.11b}$$

In this Section we concentrate on the overdamped, (2.10), and underdamped behaviour, (2.11), of η_1.

$\varkappa$ can be easily related to η_1. First of all ω_A, ω_B and ΔV in eqs (2.10) and (2.11) must be rewritten in our notation:

$$\omega_A^2 = \omega_B^2 = \gamma\alpha \, , \qquad \Delta V = 2\gamma\alpha \, . \tag{2.12}$$

Furthermore we notice that: (i) there are two escape paths at $\vartheta = -\pi$ and $\vartheta = \pi$/11/; (ii) the potential minima are bistable, ie the probability flux can cross the barriers inwards; (iii) whenever the brownian particle crosses a barrier, for instance at $\vartheta = \pi$, as an effect of the potential periodicity

(M=1), it is like as it falls inside through $\vartheta = -\pi$. Each feature mentioned above speeds up the re-equilibration process by increasing the relaxation rate by a factor 2 each, so that

$$\varkappa = \delta \eta_1 . \qquad (2.13)$$

Mechanisms (i) and (ii) are well understood, while (iii) is peculiar to our model. The effects due to (iii) can be computed directly in the overdamped limit on employing the mean-first-passage-time technique /17, 18/. The time τ_e needed for the brownian particle to reach the bottom of a neighbouring well (for instance $\vartheta = 2\pi$) starting out at $\vartheta = 0$ is given by:

$$\tau_e = \frac{\beta}{\alpha^2} \int_0^{2\pi} e^{-\gamma/\alpha \cos\theta} d\theta \int_0^{\vartheta} e^{\gamma/\alpha \cos\phi} d\phi . \qquad (2.14a)$$

τ_e can be readily recast as:

$$\tau_e = \frac{\beta}{\alpha^2} \int_{-\pi}^{\pi} e^{\gamma/\alpha \cos\theta} d\theta \int_{-\pi}^{\vartheta} e^{-\gamma/\alpha \cos\phi} d\phi , \qquad (2.14b)$$

and on integration by parts and some simple algebra:

$$\tau_e = \frac{\beta}{2\alpha^2} \left[\int_{-\pi}^{\pi} e^{\gamma/\alpha \cos\theta} d\theta \right]^2 = \frac{\beta}{2\alpha^2} \left[2\pi I_0(\gamma/\alpha) \right]^2 . \qquad (2.15)$$

I_0 is a Bessel function and for $\gamma \gg \alpha$ can be approximated so as to yield the expected result

$$\tau_e^{-1} = 2\eta_1 \qquad (2.16)$$

where η_1 is that of eq (2.10). The same result is recovered in the underdamped limit on adopting an appropriate approach for small viscosities /19/.

We are now in a position to compare the results of the numerical algorithm for the translational diffusional constant D, eq (2.2), with our predictions, $\varkappa$, based on the Kramers' theory (eq (2.13) and eqs (2.10) and (2.11)). For computational convenience we only report numerical results for $C_{del}(t)$ obtained on assuming delta function initial conditions eq (1.6), with $\omega_0 = 0$. This is the case usually studied in the literature via computer simulation /16-18/. As shown in ref 20 the differences between $C_{eq}(t)$ and $C_{del}(t)$ concern the short-time behaviour only, so that the reported results for μ are to be regarded as very close to the actual values for the particle mobility. In particular we note that (i) the derivation of eq (2.1) is still valid under delta function initial conditions provided that $\omega_0 = 0$; (ii) the linear approximations of eq (2.3)-(2.9) do not depend on the initial conditions; (iii) on the limit $\gamma \gg \alpha$, the escape rate η_1, eqs (2.10) and (2.11), is not appreciably affected by the choice of $\rho(\vartheta, \omega; 0)$ since the hopping phenomenon is a long-time process. Corrections due to the different initial conditions can be estimated analytically /20/. Finally, all these statements have been checked numerically by comparing $C_{eq}(t)$ and $C_{del}(t)$ for several relevant choices of the model parameters /8/.

In the limit of high barriers ($\gamma \gg \alpha$) the agreement with the theoretical predictions is very satisfactory both in the overdamped and underdamped limit. In fig 1 we display D and $\varkappa$ versus γ for M = 1 and $\beta = 10$. A large discrepancy between $\varkappa$ and D occurs as expected at small values of γ, where D tends to the correct 'Debye's limit' α^2/β (see Section 3). In fig 2 we present our results for the underdamped regime (M = 1, $\gamma = 10$). A linear dependence on β is achieved; the slope of the straight line fitting to our numerical points resembles more closely that predicted by Bütticker et al /16/, (2.11b), compared to the earlier estimate due to Kramers /12/, (2.11a). Our results provide an evidence for the validity of the theoretical arguments supporting the refined version of Kramers' approach /16, 21/.

The ability of the activation rate theory to determine the static mobility (for M = 1) for the entire range of friction coefficient is the main result of the present Section. Claims about the breakdown /1/ of the

Kramers' theory by some authors /1,2/ are due to the inaccuracies in their algorithm, and their application of the theory to the problem under study.

(b) dynamic mobility

In this paragraph we illustrate some results for the dynamical mobility, eq (1.8), which cannot be explained in terms of the derivations leading to eqs (2.3) and (2.9) based on linear approximations. The nonlinear nature of the external potential $V(\vartheta)$ is shown to play a dominant role in explaining the spectrum of $C_{del}(t)$ (or $C_{eq}(t)$).

In figs 3-5 we observe a behaviour similar to that detected by Dieterich et al /1/ in the range of relatively small friction coefficient $\beta = 0.05$. At $\gamma = 2$, a strong oscillatory peak appears approximately at the resonance frequency (figs 3 and 5):

$$\Omega_0 = \sqrt{\gamma \alpha} \tag{2.17}$$

(see eqs (2.5)-(2.7)). At $\gamma = 1$ the spectrum of $\hat{C}_{del}(s)$ in fig 3 is dominated by a central peak, reflecting the diffusional character of the brownian motion inside the well (see also fig 5). At an intermediate temperature $\gamma = 1.4$, a pronounced minimum shows up in $\hat{C}_{del}(s)$ near $s = 0.5\Omega_0$. In fig 4 the position of $\hat{C}_{del}(s)$ maxima is plotted versus γ for $\beta = 0.05$. The dashed region corresponds to the simultaneous presence of two maxima. For $\beta > 0.2$ the transition between the oscillatory and the diffusive regime takes place without the appearance of a minimum at finite s.

Such a behaviour cannot be explained in terms of the analysis in the linear approximation of Section 2a. Indeed for $\hat{C}_L(s)$ in eq (2.9) we observe either a central or an oscillatory peak but do not observe both peaks simultaneously. To fully account for the features of the spectrum of $C_{del}(t)$ we should therefore be able to include the effects due to the non-linearity

Effects due to non-linearity are shown clearly on analyzing $\mu(\omega)$ in more detail. Fig 5 shows that the dynamic mobility presents appreciable substructures especially around $2\Omega_0$. These are better resolved in fig 6. A natural explanation consists of tracing back the new peaks to a (nonlinear) harmonic structure. A more refined discussion of the resonance dynamics of the model lies outside the purview of our investigation. We remark that a qualitative support to our interpretation comes from the similar fine structure of the orientational acf spectrum (see Sections 3 and 4).

3 DIELECTRIC LOSS

In this Section we examine the effects due to the multiwell structure of the periodic potential $V(\vartheta)$ $(M>1)$. By simply changing variables $\vartheta \to M\vartheta$ in eq (1.1) we realize that the angular velocity rotational acf can be obtained from the case with M = 1 on having rescaled $\alpha \to M\alpha$ and $\gamma \to M\gamma$. This argument does not apply to $K_{eq}(t)$, From eq (1.10), $\varepsilon''(\omega)$ is obtained as below:

$$\varepsilon''(\omega) = (\varepsilon_s - \varepsilon_\infty)\,\omega\, Re\left\{ \int_0^\infty e^{-i\omega t} \langle \cos\vartheta(t)\cos\vartheta(0)\rangle_{eq}\, dt \right\} . \qquad (3.1a)$$

The coefficient $\varepsilon_s - \varepsilon_\infty$ depends on the dielectric system under study and is not accounted for in our model /15/. It should therefore be regarded as a free normalization parameter when a comparison of the model predictions with experimental data is carried out / 8/. In view of easy properties of Fourier transformation we can rewrite eq (3.1a) for $\varepsilon''(\omega)$, apart from a new arbitrary normalization coefficient,

$$\varepsilon''(\omega) = \omega\, Re\left\{ \int_0^\infty e^{-i\omega t} K_{eq}(t)\, dt \right\} \qquad (3.1b)$$

with $K_{eq}(t)$ defined in eq (1.10).

Our analysis yields results roughly similar to those derived analytically under several assumptions by Praestgaard and van Kampen /11/. Under some restrictions the short-time behaviour of the brownian motion in an M-fold potential arises entirely from the motion bounded inside a single well (resonance or libration), while long-time dynamics is dominated by the hopping of the brownian particle over the barriers. The latter phenomenon is shown to produce a purely diffusional behaviour for $K_{eq}(t)$, which becomes dominant for high activation energies ($\gamma \gg \alpha$). This implies that irrespective of the dynamics inside a single well, the relaxational process for $M>1$ is governed by the slow diffusion over the potential barriers. The activation time of this mechanism corresponds to an effective time scale for the relaxational process. A marked difference in the relaxational behaviour is therefore expected between the single well and the multiwell cosine potential (see Appendix B).

These ideas are quantified on giving an approximate analytical expression for $K_{eq}(t)$. This is obtained from the analytical results of Praestgaard and van Kampen. First of all we recall that for the brownian motion in a paraboli potential, $V(\vartheta) = \Omega_0^2 \vartheta^2/2$ $(\Omega_0^2 = \gamma\alpha)$, the corresponding orientational acf, $K_L(t)$, is given by:

$$K_L = \frac{\cosh\left[\frac{\alpha}{\gamma}\, \mathcal{U}_\omega(t)\right] - 1}{\cosh\frac{\alpha}{\gamma} - 1} , \qquad (3.2)$$

where $\mathcal{U}_\omega(t)$ is as in eq (2.5). In the limit of free relaxation $(\gamma \to 0)$ we obtain:

$$\underset{\gamma=0}{K}(t) = \lim_{\gamma\to 0} K_L(t) = \exp\left[-\frac{\alpha^2}{\beta^2}\left(-1 + \beta t + e^{-\beta t}\right)\right] . \qquad (3.3)$$

$\hat{K}_{\gamma=0}(s)$ can be written in terms of a continued fraction expansion/10/:

$$\hat{K}_{\gamma=0}(s) = \cfrac{1}{s + \cfrac{\alpha^2}{s+\beta + \cfrac{}{\ddots + \cfrac{n\alpha^2}{s + n\beta + \ddots}}}} . \qquad (3.4)$$

The corresponding diffusional constant is then defined as the inverse of $\hat{K}_{\gamma=0}(0)$, and for large friction $(\beta \gg \alpha)$ is approximated by

$$\hat{K}_{\gamma=0}(0) \underset{\beta\gg\alpha}{\sim} \frac{\beta}{\alpha^2} , \qquad \text{('Debye time')} . \qquad (3.5)$$

This result coincides with that for D for $\gamma = 0$, computed in Section 2 (fig 1).

Following the procedure outlined in ref 11 (see Appendix B), we find our approximate expressions for the normalized orientational acf's:

$$K_{eq}(t) = e^{-\varkappa_1 t} \; K_L(t) \qquad (M = 1), \qquad (3.6)$$

$$K_{eq}(t) = e^{-\varkappa_2 t} \; \frac{\cosh \alpha/\gamma - 1}{\cosh \alpha/\gamma} \; K_L(t) + \frac{e^{-2\varkappa_2 t}}{\cosh \alpha/\gamma} \qquad (M = 2). \qquad (3.7)$$

We note immediately that in the limit of large barrier height ($\gamma \gg \alpha$) the first term on the r.h.s. of eq.(3.7) vanishes. A purely diffusional (long-time) term then describes the relaxation in a multi-well periodic potential. The $\gamma/\alpha \to \infty$ limit of $K_{eq}(t)$ for any $M > 1$ is given by/11/:

$$K_{eq}(t) \underset{\gamma \gg \alpha}{\sim} \exp\left[- \varkappa_M \left(1 - \cos \frac{2\pi}{M} \right) t \right] . \qquad (3.8)$$

$\varkappa_M$ is to be related to the Kramers' activation rate η_M for an M-fold cosine potential. From ref 11:

$$\varkappa_M = 2 \eta_M \qquad (M > 1),$$

while η_M can be obtained from eqs (2.10) and (2.11) with $\omega_A^2 = \omega_B^2 = M^2 \gamma \alpha$.

For the case M = 1 the short-time contribution proportional to $K_L(t)$ fully describes the relaxational process. Increasing the height of the barrier ($\gamma \gg \varkappa$), the motion inside the well becomes strongly oscillatory as the resonance frequency, eq (2.17), being proportional to $\sqrt{\gamma}$, becomes much greater than β. The behaviour of $K_{eq}(t)$ for M = 1 and $M > 2$ is therefore expected to be markedly different.

In fig 7 we report the frequency of the maxima of $\varepsilon''(\omega)$ for the case M = 1. The overdamped and underdamped regimes are clearly distinguishable. Indeed from eqs (3.6) and (3.2) in the limit $\gamma \gg \alpha$, $K_{eq}(t)$ can be approximated as

$$K_{eq}(t) \underset{\gamma \gg \alpha}{\sim} U_\omega^2(t) . \qquad (3.9)$$

From eq (2.5) we find the following two asymptotic behaviours

$$K_{eq}(t) \underset{\gamma \gg \alpha}{\sim} \begin{cases} \frac{1}{2} e^{-\beta t} \left(1 + \cos 2\Omega t \right), & \beta \ll \Omega_o, \qquad (3.10a) \\ e^{-2\frac{\Omega_o^2}{\beta} t}, & \beta \gg \Omega_o . \qquad (3.10b) \end{cases}$$

$\varepsilon''(\omega)$ can now be computed explicitly using eq (3.1b). We find that in the overdamped limit, (3.10b), only one (diffusional) loss peak arises around $2\Omega_o^2/\beta$. In the underdamped limit we still have a diffusional peak on the left hand side of the spectrum around β, however a more pronounced, sharp librational peak shows up at high frequency around 2Ω (see also fig 8). The discussion for the analytical expressions explains the numerical results of fig 7.

Now we present some results for M = 2 Our algorithm works quite well for M> too. By choosing M = 2 we do not imply for the amount that this is a suitable choice for fitting experimental data on dielectric relaxation (the usually adopted multplicity M lies between 8 and 12). The case M = 2 is relevant, however, to several studies of the dipole-dipole

interaction in the presence of external noise/10/. The conclusions reported below are to be regarded valid for any M.

In fig 9, we show the position of the loss peak ω_m versus β. For $\gamma = 4$, the librational contribution to $K_{eq}(t)$ (eq (3.7)) is ma e almost negligible (see also fig 8). For this case, we find readily that ω_m is centred approximately at $2\varkappa_2$. As explained in Section 2, $\varkappa_2$ is related to the Kramers' escape rate η_2 - hence $\omega_m \sim 4\eta_2$. Our numerical results for ω_m are compared with an accurate theoretical estimate, ω_m^{th}. This has been obtained by bridging the rate η_2 in eq (2.10), valid for large to intermediate viscosity, with the expression for the small to intermediate viscosity, η_2^{BHL}, of ref 16:

$$\omega_{m_2} = 4\left[\eta_2^{-1} + (\eta_2^{BHL})^{-1}\right]^{-1}, \tag{3.11}$$

where

$$\eta_2^{BHL} = \frac{\left[\left(1+2\sqrt{\alpha/\gamma}\ \alpha/\beta\right)^{1/2}-1\right]}{\left[\left(1+2\sqrt{\alpha/\gamma}\ \alpha/\beta\right)^{1/2}+1\right]}\ \frac{8\gamma}{\alpha\pi}\ e^{-2\gamma/\alpha} \tag{3.12}$$

An almost complete agreement between the theoretical estimates and the numerical results is a further proof of the validity of the theoretical approach developed in ref 16, in combination with our results for $\varkappa_2$.

4. CONCLUSIONS

The mobility of a particle, $\mu(\omega)$, and complex permittivity, $\varepsilon^*(\omega)$, of a system of dipolar molecules undergoing rotational brownian motion in an M-fold cosine potential are given in Sections 2 and 3 respectively. In spite of the non-linear effects reported in Section 2, yet the approximation of $V(\vartheta)$ to a set of M parabolic wells is shown to reproduce most of the diffusional features for both the rotational and orientational a.c.f.'s. In particular we find that the diffusion coefficient is related to the Kramers' escape rates over the entire range of the friction coefficient. The numerical results of Reid's algorithm allow us to determine the activation rates for the underdamped limit which agree closely with a recent refinement of Kramers' work (Sections 2 and 3). An important conclusion of Section 3 is that the hopping dynamics in a multiwell potential determines the relaxation behaviour irrespective of the friction coefficient.

The present work has dealt with mainly the relaxation behaviour of the brownian motion in a cosine potential. The librational features of the frequency spectrum for $\langle w(t)w(0)\rangle$ and $\langle\cos\vartheta(t)\cos\vartheta(0)\rangle$ could be investigated in a subsequent paper. We note, from the specturm of $\mu(\omega)$, that a second peak appears at the 2nd harmonic of the oscillator frequency, due to the non-linearity in the model. In fig. 8 (see also discussion for M = 1 in Section 3) a librational substructure appears on the r.h.s. of the loss peak. This feature is enhanced in the spectrum of the power absorption $\alpha(\omega)$, eq (1 A finer structure of peaks is superimposed on the usual (sub)-harmonic struct detected in $\mu(\omega)$. It may be emphasized here that this finer structure (fig 10) of peaks in $\alpha(\omega)$ especially for low β is not due to the characteristics of a non-linear deterministic oscillator. These may be att to the stochastic molecular dynamics in a non-linear potential and are important numerical predictions of this model. The reliability of the presen model to interpret the far infrared spectroscopy of dielectrics is an outstar problem. To apply the one-dimensional cosine model to a dielectric system,

we must determine the crucial parameters, M, γ and β. The parameter β can reasonably be assumed to be proportional to the macroscopic viscosity (hydrodynamic hypothesis). However we do not know whether β is to be taken small (underdamped limit) or large (overdamped limit). From experiments, however, we find that the frequency of maximum $\varepsilon''(\omega)$ decreases with an increase in viscosity and thus ω_m lies along the decreasing branch of the curve in fig. 9. It follows therefrom that a comparison of the model with the experiment is meaningful for large values of β only and possibly for M lying between 8 and 12. For the case $\alpha < \beta$ and for low γ, a linear dependence of dielectric relaxation time on viscosity is found, eq (3.5), as for the Debye's model.

A puzzling experimental feature of delectrics is that a dielectric system with strong dipole-dipole coupling exhibits a single relaxation time whereas a dilute solution of these systems gives rise to a distribution in the relaxation times /22/. This leads to a half-width of $\varepsilon''(\omega)$ of almost 1.14 decades for systems with strong coupling (like n-alcohols and water) /23/ whereas a broad $\varepsilon''(\omega)$ curve for dilute solutions of n-alcohols in heptane (weak coupling)/24/. This paradoxical feature can now be explained by this model. For $\gamma > \alpha$, we find from eq. (3.8) that $K_{eq}(t)$ is an exponential decay function of time. The corresponding expression for $\varepsilon''(\omega)$ is :

$$\varepsilon''(\omega) = \frac{\sigma \omega}{\omega^2 + \sigma^2} \qquad (4.1)$$

with $\sigma = 2 \eta_M \left(1 - \cos \frac{2\pi}{M}\right)$.

This implies that the half-width of the $\varepsilon''(\omega)$ curve is proportional to η_M (eq. (2.10), for large β). η_M decays exponentially with an increase in γ. Hence the half-width of the dielectric loss peak is dependent on γ (height of the potential barrier or magnitude of the dipole-dipole coupling). This suggests a satisfactory explanation for the experimental observation.

Finally we may emphasize that the results reported here can be extended to other fields of condensed matter. In particular, the frequency dependence of the mobility spectrum of a superionic conductor is explained successfully by the periodic cosine potential. The model yields results for the diffusion coefficient (related to the static mobility) over a range of the values of the friction coefficient. This can explain the dependence of mobility on the impurity concentration in a semiconductor. The dependence of current on the capacitance and resistance of the Josephson's junction for an extremely undamped case, can also be explained.

ACKNOWLEDGEMENTS

We are grateful to Professor B K P Scaife for useful discussions.

Mr D Simpson is thanked for the drawings.

APPENDIX A

The main features of Reid's algorithm /8/ are summarized as follows. The solution of eq (1.4) is assumed to be of the form

$$f(\vartheta,\omega;t) = \exp\left(-\omega^2/4\alpha^2\right)\sum_{n=0}^{\infty} H_n(\omega/\alpha)\,\phi_n(\vartheta;t) \quad , \tag{A.1}$$

where $H_n(x)$ is the n-th orthogonal Hermite polynomial and the spatial dependence $\phi_n(\vartheta;t)$ may be expanded into a Fourier series

$$\phi_n(\vartheta;t) = \sum_{p=-\infty}^{+\infty} A_p^n(t)\exp(ip\vartheta) \quad . \tag{A.2}$$

On substituting eqs (A.1) and (A.2) into (1.4) we easily obtain the set of differential-differences equations /9, 10/:

$$\dot{A}_p^n(t) + n\beta A_p^n(t) - iM\gamma/2\left(A_{p-M}^{n-1}(t) - A_{p+M}^{n-1}(t)\right) + ip\alpha\left(A_p^{n-1}(t) + (n+1)A_p^{n+1}(t)\right) = 0 \quad . \tag{A.3}$$

It is convenient to define normalized sums and differences of coefficients by

$$S_p^n(t) = \left(A_{-p}^n(t) + A_p^n(t)\right)/2A_o^o(0) \quad , \tag{A.4}$$

$$D_p^n(t) = \left(A_{-p}^n(t) - A_{-p}^n(t)\right)/2A_o^o(0) \quad . \tag{A.5}$$

Further, if the set of eqs (A.3) are rewritten in terms of S_p^n and D_p^n and then Laplace transformed ($\mathcal{L}\{S_p^n(t)\} \equiv \hat{S}_p^n(s)$) into algebraic equations it is found that the differences can be eliminated to leave a recurrence relation which, in turn, may be written as an algebraic matrix equation /8/:

$$\underline{\underline{A}}\;\underline{\hat{S}}_p^n(s) = S_p^n(0) \quad . \tag{A.6}$$

The elements of $\underline{\underline{A}}$ are function of s and of the parameters α, β, γ and M. The vector $\underline{S}^n_p(0)$ contains the initial conditions and in general depends on both $S^n_p(0)$ and $D^n_p(0)$. For delta function initial conditions, eq (1.6), the elements of $\underline{S}^n_p(0)$ coincide with $S^n_p(0)$, ie

$$S^n_p(0) = \exp\left(\omega_0^2/4\alpha^2\right) H_n\left(\omega_0/\alpha\right) \cos(p\vartheta_0)/n! \quad . \qquad (A.7)$$

To solve (A.6), we restrict the number of equations (A.3) by assuming $\hat{S}^n_p(s) \equiv 0$) for $n > N$ (up to 50) or $p > P$ (up to 100). The consequent numerical inversion of $\underline{\underline{A}}$ yields a very accurate solution for $\hat{S}^n_p(s)$.

$S^1_0(t)$ is readily related to the angular velocity acf by :

$$\langle \omega(t)\omega(0)\rangle_0 / \langle \omega^2(0)\rangle_0 = S^1_0(t)/S^1_0(0) \qquad (A.9)$$

Similarly we find that

$$\langle \cos\vartheta(t)\cos\vartheta(0)\rangle_0 / \langle \cos^2\vartheta(0)\rangle_0 = S^0_1(t)/S^0_1(t) \qquad (A.10)$$

If $\langle\ldots\rangle_0$ denotes delta function initial conditions $\hat{S}^1_0(s)$ and $\hat{S}^0_1(s)$ are solution to the algorithm of eqs (A.6) and (A.7). The corresponding equilibrium acf's, $\langle\ldots\rangle_{eq}$, are then obtained by assuming ϑ_0 and ω_0 distributed according to the corresponding Maxwell-Boltzmann probability function (1.7). It corresponds to solving the set of equations (A.6) by using $\langle\omega(0)\, S^n_p(0)\rangle_{eq}$ and $\langle\cos\vartheta(0)\, S^n_p(0)\rangle_{eq}$ respectively, instead of $S^n_p(0)$ /8/.

APPENDIX B

In this Appendix we report some results of ref 11. Firstly, the definition of acf for the physical observable A(t) is

$$\langle A(t)A(0)\rangle = \int \rho(\vartheta_0\omega_0;0)\, A(0)\, d\vartheta_0 d\omega_0 \int \rho(\vartheta,\omega;t|\vartheta_0\omega_0;0)\, A(t)\, d\vartheta(t) d\omega(t) \qquad (B.1)$$

where the transition probability density $\rho(\vartheta,\omega;t|\vartheta_0\omega_0;0)$ coincides with the solution $\rho(\vartheta,\omega;t)$ of the FPE (1.4) with delta function initial conditions, (1.6). The equilibrium acf's, $\langle\ldots\rangle_{eq}$, are obtained by using the Maxwell-Boltzmann distribution $\rho_{eq}(\vartheta_0,\omega_0)$ for ϑ_0 and ω_0 in eq (1.7).

In the linear approximation (Section 2) of potential

$$V(\vartheta) = \frac{1}{2}\gamma\alpha\vartheta^2 , \qquad (B.2)$$

$\rho(\vartheta,\omega;t)$ is gaussian and has been obtained explicitly in ref 13. In particular, the first moments of this gaussian are given by the solution of the damped harmonic oscillator:

$$\begin{pmatrix} \langle\vartheta(t)\rangle \\ \langle\omega(t)\rangle \end{pmatrix} = \begin{pmatrix} \mathcal{U}_\vartheta(t) & \mathcal{U}_{\vartheta\omega}(t) \\ \mathcal{U}_{\omega\vartheta}(t) & \mathcal{U}_\omega(t) \end{pmatrix} \begin{pmatrix} \vartheta_0 \\ \omega_0 \end{pmatrix} \qquad (B.3)$$

with

$$\mathcal{U}_{\vartheta\omega} = e^{-\frac{\beta}{2}t} \sin(\Omega t)/\Omega ,$$

$$\mathcal{U}_{\omega\vartheta} = -e^{-\frac{\beta}{2}t} \gamma\alpha \sin(\Omega t)/\Omega , \qquad (B.4)$$

and Ω, $\mathcal{U}_\vartheta$ and $\mathcal{U}_\omega$ introduced in eqs (2.5)-(2.7). On substituting A(t) in eq (B.1) with $\vartheta(t)$ and $\omega(t)$, the expressions (2.3) and (2.4) for $R_L(t)$

and $C_L(t)$ respectively are easily obtained. (In the parabolic approximation no escape over potential barriers can occur, ie $\varkappa = 0$). $K_L(t)$ given by eq (3.2) is also obtained in ref 11 (eqs (12) and (21)), on adopting Chandrasekhar's solution for the second moment of $p(\theta, \omega, t)$ /13/.

An M-fold cosine potential with high barriers ($\gamma >> \varkappa$) is approximated in ref 11 by a replica of parabolic potential wells, eq (B.2), for $|\theta| < \pi/M$. Each of these wells is centred at a cosine potential minima $\Theta_\nu = \frac{2\pi}{M}\nu$ ($\nu = 0, \ldots M-1$). The relaxational dynamics of the variable $\omega(t)$ can then be reduced to the case M = 1 (Section 3). On the contrary, the acf's for $A(\vartheta(t))$ are to be treated cautiously due to the relevance of the M-fold potential structure.

The equilibrium acf's of observables depending on $\vartheta(t)$ are separated by Praestgaard and van Kampen into a short-time, S(t), and a long-time term, L(t), ie

$$\langle A(t)\, A(0)\rangle_{eq} = S(t) + L(t). \tag{B.5}$$

(a) The short-time term, S(t) - If the planar rotator starts out in the potential well around Θ_ν at time t = 0, the probability that at time t > 0 it is still librating inside the ν-th well is:

$$p(t) = e^{-\varkappa t} \tag{B.6}$$

where the appropriate escape rate, $\varkappa$, is independent of ν due to the similarity between the various potential minima. In Sections 2 and 3, $\varkappa$ is related to the Kramers' escape rate for any M. In the Praestgaard and van Kampen approximation for $V(\vartheta)$, S(t) is obtained by the application of eq (B.1) to an M-fold harmonic potential with a probability normalization constant dependent on time, (B.6):

$$S(t) = \frac{p(t)}{M} \sum_\nu \langle A(\Theta_\nu + \vartheta(t))\, A(\Theta_\nu + \vartheta(0))\rangle . \tag{B.7}$$

Eq (B.7) reduces to

$$S(t) = p(t)\, \langle A(t)\, A(0)\rangle_L \tag{B.8}$$

for M = 1 and 2. Here $\langle \ldots \rangle_L$ denotes the corresponding acf for the linear case. It is interesting to note that eq (B.8) is not valid for M > 2. In fact for M = 1, eq (B.8) follows immediately from the usual linear approximation and is valid for high barriers only. For M = 2, the two potential wells are symmetric, the evolution of $A(\vartheta(t))$ inside either of the wells is indistinguishable from each other. The resultant formula for M = 2 is therefore the same as for M = 1 except that $\varkappa$ values are different for the two cases. It may be noted that equation (B.8) follows after making corrections for minor mistakes in eqs (36) to (39) of ref 11.

When A(t) is $\vartheta(t)$ or $\cos\vartheta(t)$, eqs (2.4) and (3.6) and the first term on the rhs of eq (3.7) are readily obtained.

(b) The long-time term, L(t) - For M > 1 the hopping phenomenon plays a major role in the relaxation of $A(\vartheta(t))$. Following ref 11 this mechanism is illustrated by introducing a probability $P_\nu(t)$ for the rotator to be in the ν-th well at time t and also a transition probability $W(\nu \to \mu, t)$, $\mu \neq \nu$, (defined as the probability that it makes its first jump between t and t + dt ending up in the μ-th well). For determining the equilibrium statistical properties of the system, the rotator is assumed to lie at the bottom of a potential well Θ_ν with probability $P_\nu^{eq} = 1/M$. L(t) is then

given by

$$L(t) = \sum_{\substack{\nu,\mu \\ \nu \neq \mu}} P_\nu^{eq} A(\Theta_\nu) \int_{-t}^{0} w(\mu \to \nu, t') A(\Theta_\mu) P_\mu(t+t') dt' \qquad (B.9)$$

On making explicit calculations for $w(\mu \to \nu, t)$ and $P_\nu(t)$ /11/ and on replacing $A(t)$ with $\cos\vartheta(t)$, the long-time contributions to $K_{eq}(t)$, eqs(3.7) and (3.8), are obtained. Note that for M =1 $w(\mu \to \nu, t)$ vanishes, hence $L(t) \equiv 0$, (see eq (3.6)). This implies that eq(2.3) for $C_L(t)$ is also valid for M > 1 after rescaling $\alpha \to M\alpha$ and $\gamma \to M\gamma$.

FIGURE CAPTIONS

Fig 1 · The overdamped limit. D/D_0 versus γ for M = 1, α = 1 and β = 10. D is defined in eq (2.2) and D_0 is its γ = 0 value (the inverse of the 'Debye time' in eq (3.5)). Our numerical results ( ) are compared with the Kramers' approximation from eq (2.10) (solid line) .

Fig 2 The underdamped limit. D versus β for M = 1, α = 1 and γ = 10. The dots represent our numerical results. The straight lines represent the theoretical predictions of eq (2.11a) (K) and of eq (2.11b) (BHL) respectively.

Fig 3 $\hat{C}_{del}(s)$ versus s/ω_0 for M = 1, α = 1, β = 0.05 and several values of γ: (a) γ = 1; (b) γ = 1.4 and (c) γ = 2. The resonance frequency ω_0 is defined in eq (2.17).

Fig 4 Position of $\hat{C}_{del}(s)$ maxima for M = 1, α = 1 and β = 0.05 at varying γ. The dashed region denotes the simultaneous existence of the relative maxima (see curve (b) of fig 3).

Fig 5 $\hat{C}_{del}(\omega)$, eq(1.9) versus ω/ω_0 for M = 1, α = 1, β = 0.05 and (a) γ = 1 and (b) $\gamma = 2.\omega_c$ is given in eq (2.17).

Fig 6 $\hat{C}_{del}(\omega)$ versus ω/ω_0 as in fig 5. Details of the second resonance peak are magnified.

Fig 7 Position of $\varepsilon''(\omega)$ peaks versus β for M = 1, α = 1 and γ = 4. $\varepsilon''(\omega)$ is defined in eq (3.1). Curves A and B represent the diffusional and librational peaks respectively in the underdamped limit. For higher friction constants we find only one loss peak (curve C). The relative approximations for A, B and C discussed in the text are reported (dashed lines). In the shadowed region peaks A and B are merging.

Fig 8 Dielectric loss, $\varepsilon''(\omega)$, eq (3.1b), for α = 1, γ = 4 and (a) M = 1, β = 0.05 ; (b) M = 1, β = 10 ; (c) M = 2, β = 1. Curves (a) and (b) are to be compared to the results displayed in fig 7.

Fig 9 The loss peak ω_m versus β for M = 2, α = 1, γ = 4. Our numerical results (o) are compared with the theoretical predictions of eq (3.11) (dashed line).

Fig 10 Power absorption α, eq (1.12), versus $\bar{\nu}$ (wave number) for M = 2, α = 2, γ = 20 and (a) β = 0.1, (b) β = 0.5

REFERENCES

[1] W. Dieterich, I. Peschel and W.R. Schneider, Z. Phys., B27, 177 (1977).

[2] W. Dieterich, I. Geisel and I. Peschel, Z. Phys., B29, 12 (1978).

[3] H. Risken and H.D. Vollmer, Z. Phys., B31, 209 (1978).

[4] H. Risken, H.D. Vollmer and H. Denk, Phys. Lett. 78A, 22 (1980); H.D. Vollmer and H. Risken, Z. Phys., B34, 313 (1978).

[5] A.J. Dianoux and F. Volino, Molec. Phys., 34, 1263 (1977).

[6] G. Grosso and G. Pastori-Parravicini, Adv. Chem. Phys., special issue 'Memory Function Approach to Stochastic Problems in Condensed Matter', eds. M.W. Evans, P. Grigolini and G. Pastori-Parravicini, to be published (1984).

[7] F. Marchesoni, Physica Scripta, 30, 19 (1984).

[8] C.J. Reid, Molec. Phys., 49, 331 (1983).

[9] H. Risken, 'The Fokker-Planck Equation; the methods of solution and applications'. Springer-Verlag (1984). Chapter 9.

[10] W.T. Coffey, M.W. Evans and P. Grigolini, 'Molecular Diffusion and Spectra', Wiley Interscience, New York, 1981. Chapter 5.

[11] E. Praestgaard and M.G. van Kampen,
Molec. Phys., 43, 33 (1981).

[12] H.A. Kramers,
Physica 7, 284 (1940).

[13] S. Chandrasekhar,
Rev. Mod. Phys., 15, 1 (1943).

[14] M.W. Evans, P. Grigolini and F. Marchesoni,
Chem. Phys. Lett., 95, 544 and 548 (1983);
F. Marchesoni and P. Grigolini,
Physica A121, 269 (1983).

[15] B.K.P. Scaife,
'Complex Permittivity, The English University Press
(1971).

[16] M. Büttiker, E.P. Harris and R. Landauer,
Phys. Rev. B28, 1268 (1983).

[17] R.L. Stratonovitch,
'Topics in the Theory of Random Noise', Gordon and Breach,
New York 1967, Vol.1, p79 and ff.

[18] P. Hänggi, F. Marchesoni and P. Grigolini,
Z. Phys. B (1984), to be published.

[19] T. Fouseca, J.A.M.F. Gomes, P. Grigolini and F. Marchesoni
Adv. Chem. Phys. (1984), to be published;
F. Marchesoni,
Adv. Chem. Phys (1985), to be published;
F. Marchesoni,
Chem. Phys. Lett. (1984), to be published.

[20] F. Marchesoni and P. Grigolini,
J. Chem. Phys., 78, 6287 (1983).

[21] P. Hänggi and U. Weiss,

[22] See e.g. H. Fröhlich,
'Theory of Dielectrics', Oxford University Press (1958),
p91.

[23] J.K. Vij, W.G. Scaife and J.H. Calderwood,
J. Phys. D14, (1981), 733.

[24] J. Crossley,
Adv. Molec. Relaxation Processes, 2, 69 (1970).

[25] C.J. Reid and J.K. Vij,
J. Chem. Phys., 79, (1983), 4624.

Fig

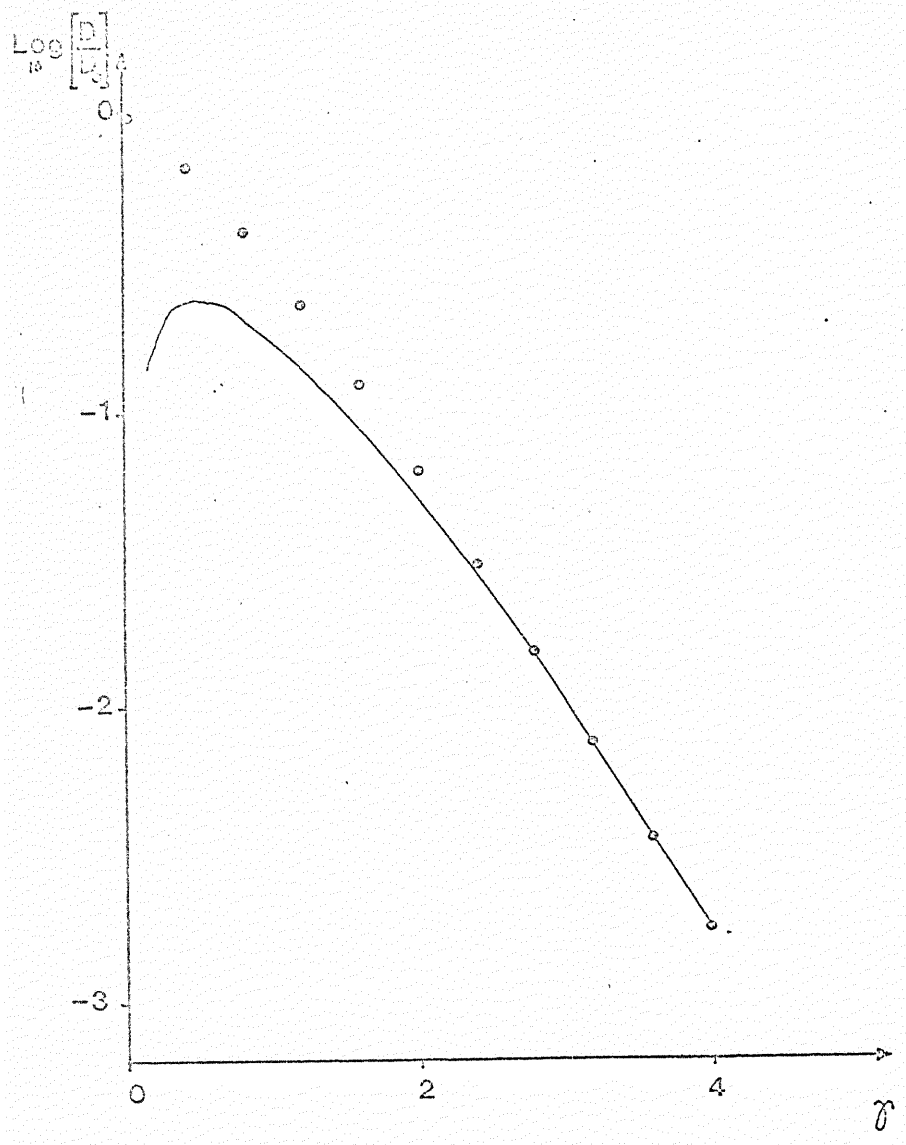

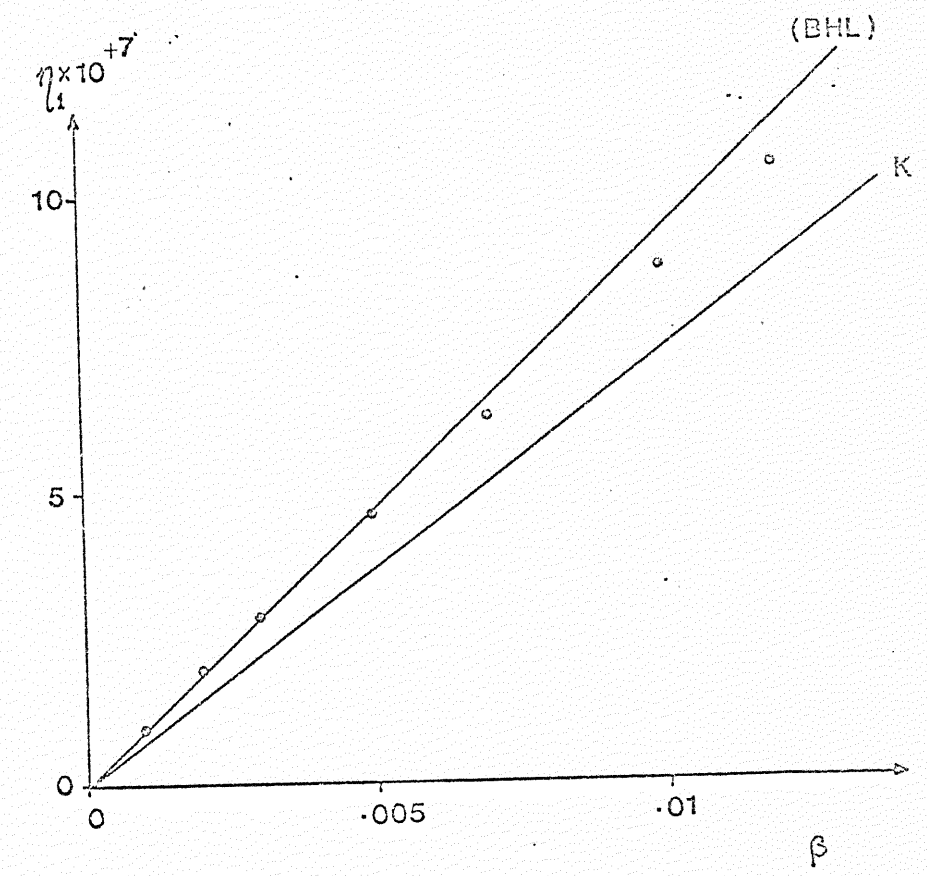

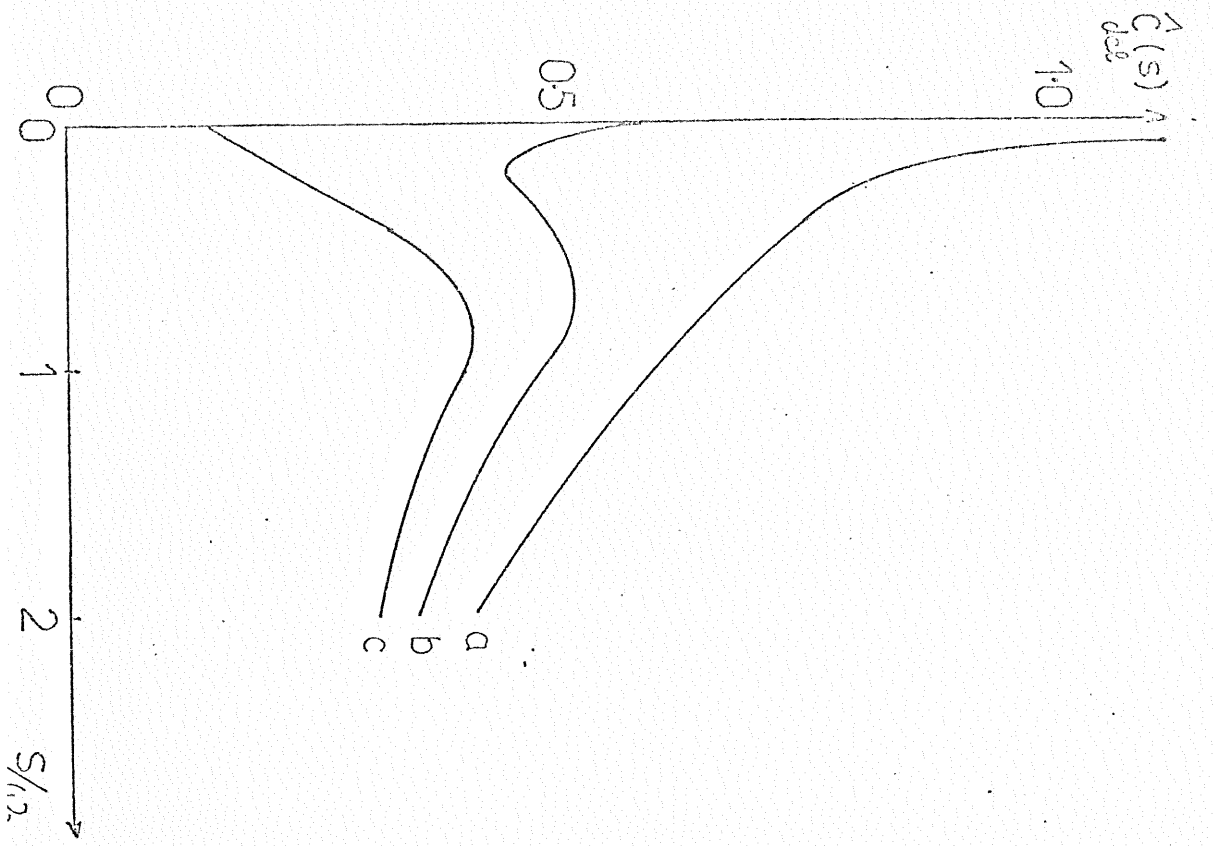

Fig 4

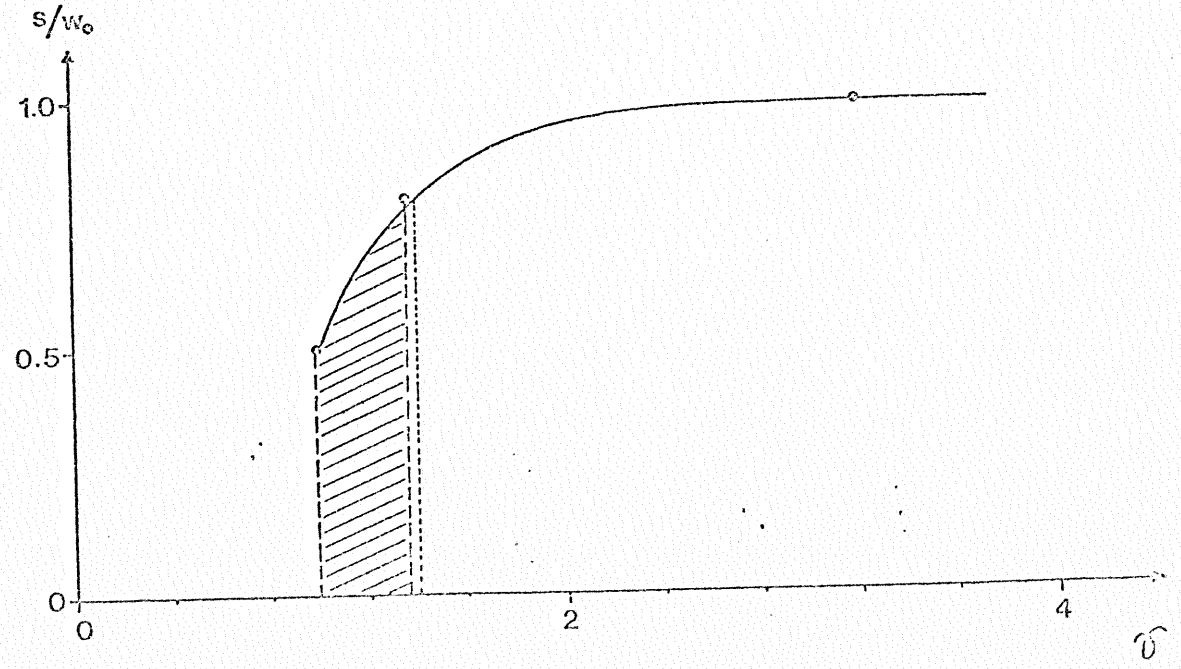

$\Lambda C_{del}(\omega)\times 10^{2}$
10·0
5·0
0
1·6
2·0
2·4
ω/ω_0
$\gamma=1$
$\gamma=2$

$\Lambda(\omega)$
0·9
0·7
0·2
a
b

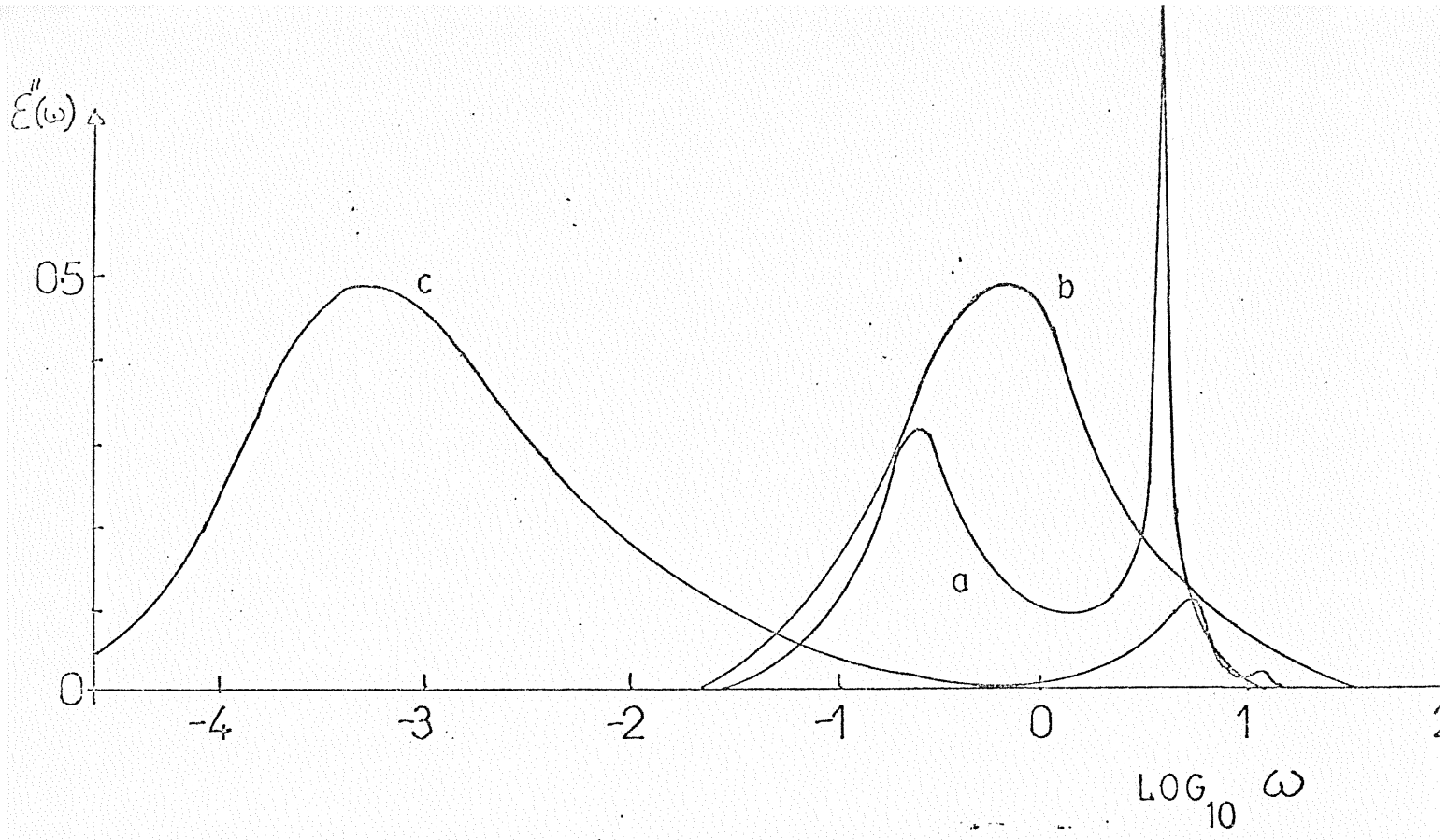
ε''(ω)
0.5
0
c
b
a
-4
-3
-2
-1
0
1
LOG10 ω

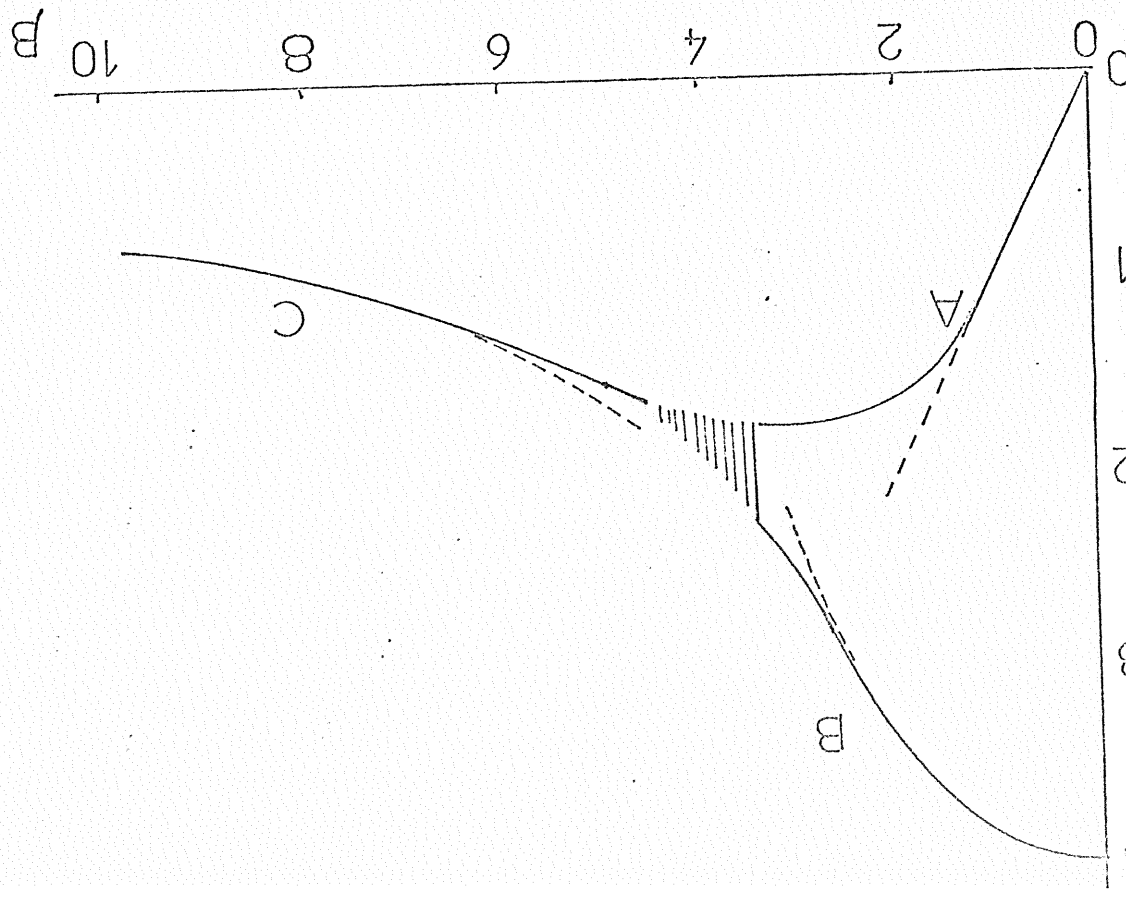
0
2
4
6
8
10
β
C
A
B

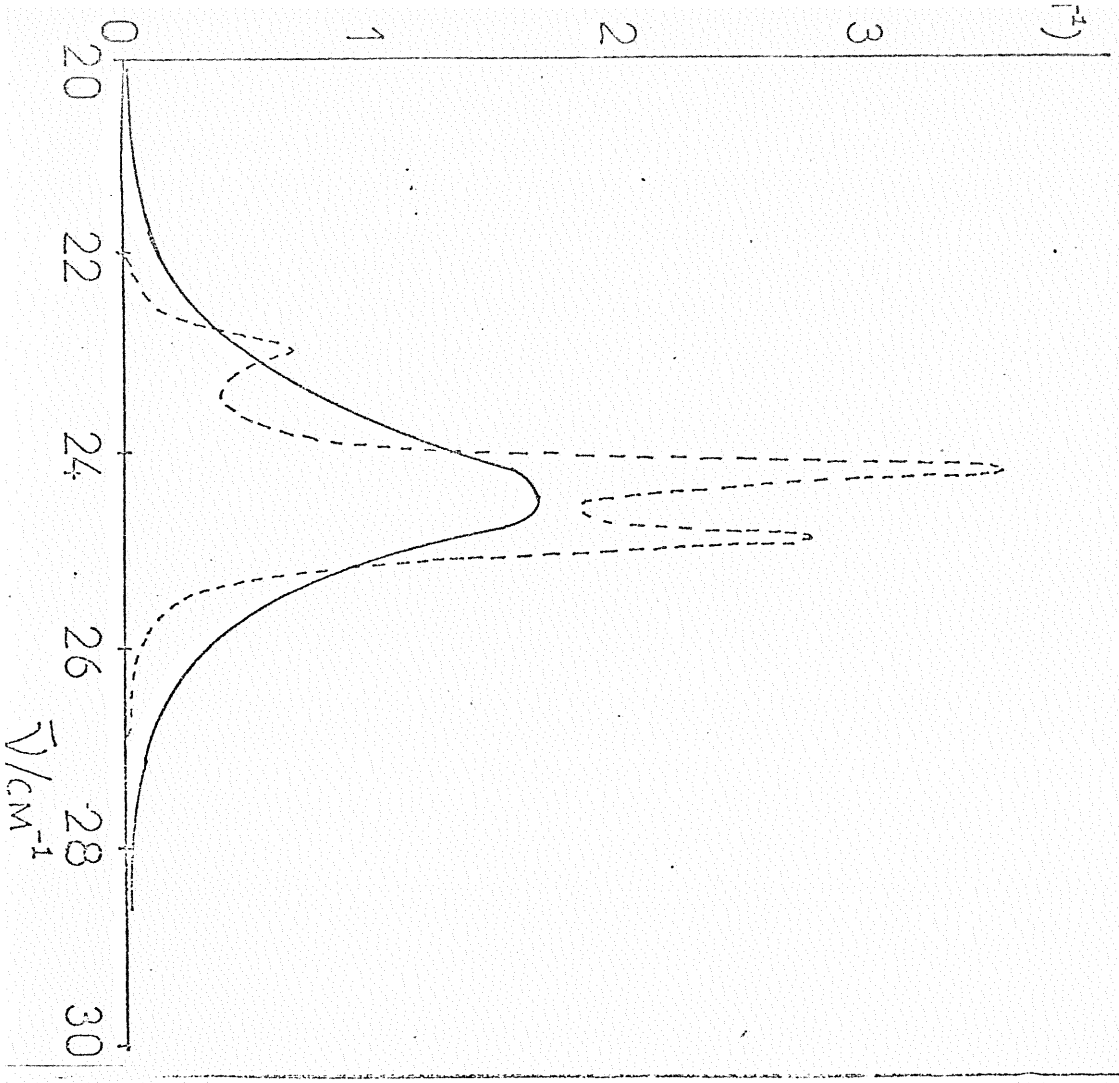
0
1
2
3
$\tilde{\nu}$/cm^{-1}
20
22
24
26
28
30

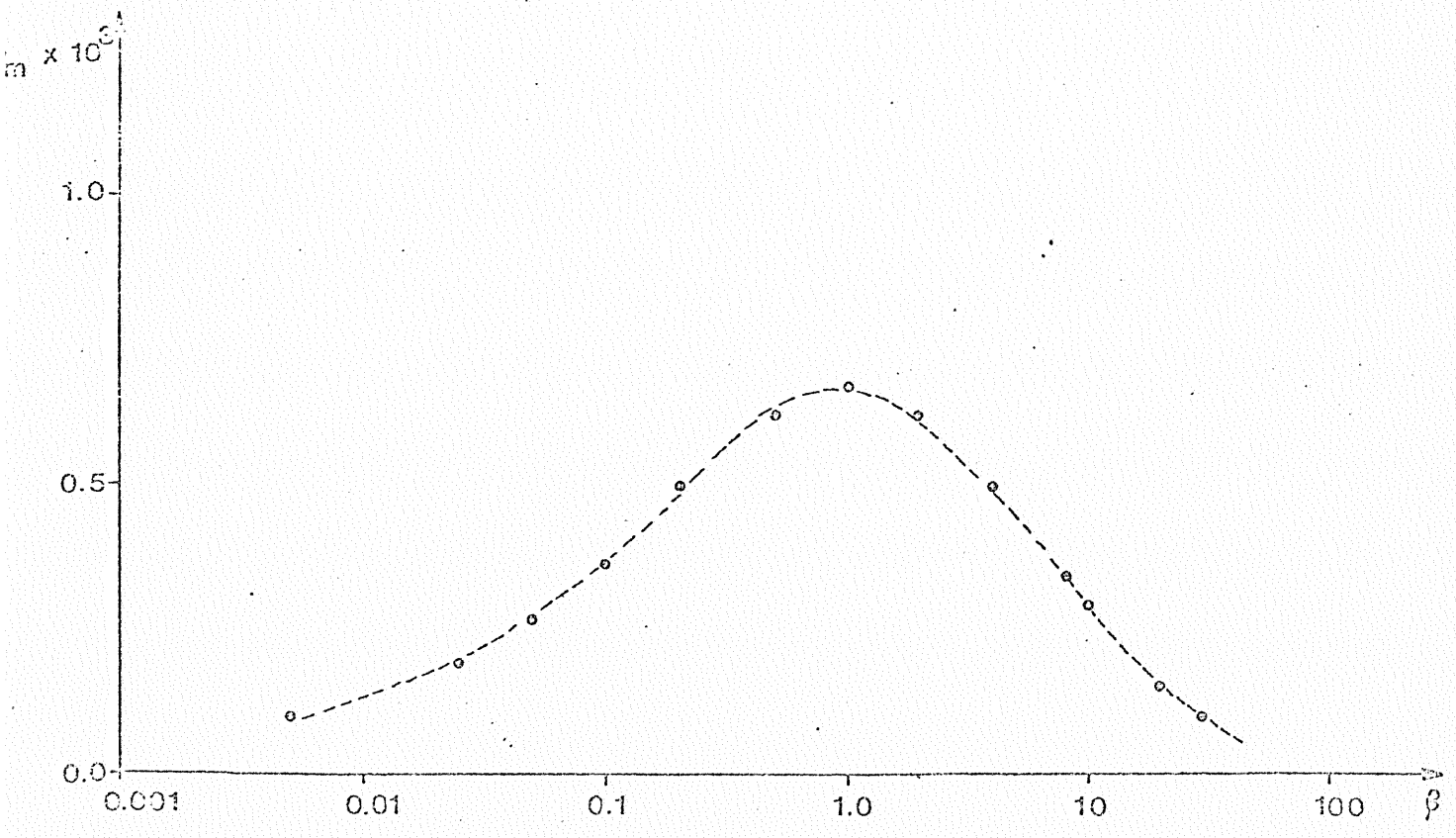
m x 10^{3}
1.0
0.5
0.0
0.001
0.01
0.1
1.0
10
100
β